Journal of Alloys and Compounds 511 (2012) 198–201

Contents lists available at SciVerse ScienceDirect

Journal of Alloys and Compounds

journal homepage: www.elsevier.com/locate/jallcom

Co_2P: A facile solid state synthesis and its applications in alkaline rechargeable batteries

Wenxiu Peng, Lifang Jiao*, Qingna Huan, Li Li, Jiaqin Yang, Qianqian Zhao, Qinghong Wang, Hongmei Du, Guang Liu, Yuchang Si, Yijing Wang, Huatang Yuan

Institute of New Energy Material Chemistry, Key Laboratory of Advanced Energy Materials Chemistry (MOE), MOE (IRT-0927), Nankai University, Tianjin 300071, PR China

ARTICLE INFO

Article history:
Received 18 June 2011
Received in revised form 6 September 2011
Accepted 6 September 2011
Available online 16 September 2011

Keywords:
Co_2P
Solid state reaction
Anode material
Alkaline rechargeable batteries

ABSTRACT

The Co_2P crystals are successfully synthesized by a facile solid state reaction. Energy dispersive X-ray spectrum (EDS) results indicate a mol ratio of 0.6686–0.3314 for Co to P, confirming the stoichiometric ratio of Co_2P. Galvanostatic charge/discharge tests show that Co_2P exhibits a high maximum discharge capacity (C_{max}) of 223.5 mAh g^{-1} and excellent cyclic properties with capacity retention of 97.9% (C_{300}/C_{max}) in the 300th cycle as an anode material in alkaline rechargeable batteries. Cyclic voltammetry (CV) and XRD tests during full charge/discharge processes confirm a quasi-reversible redox mechanism between $Co(OH)_2$ and Co resulting from the conversion of Co_2P. The simultaneously produced P plays an important role in the whole process – with the reaction and dissolution in the electrolyte, it brings many new interspaces in Co_2P body to enlarge the contact area between the active material and the electrolyte, and make the electrochemical process easier and faster.

1. Introduction

During a long time, transition metal phosphides [1–4] and supported transition metal phosphides [5–7] have been paid great attention and recognized as candidates of catalyst, because of their high activity and stability in hydrogenation, hydrodesulfurization (HDS) and hydrodenitrification (HDN) [8–10] reactions. Also, they are widely used in other fields such as electronics, optoelectronics and magnetic due to their unique physical and chemical properties [11–16]. Since Mitov et al. [17] report that Co–B amorphous alloy has electrochemical hydrogen absorption–desorption properties in alkaline rechargeable batteries, more and more efforts have been paid to investigate the electrochemical properties of various transition metal–metalloid compounds. Wang et al. [18] report Co–S alloy by ball milling of Co and S powders and obtain the highest discharge capacity of 350 mAh g^{-1} and excellent cycle stability as a negative material for Ni/MH batteries. He et al. [19] investigate the hydrogen storage performances of Co–Si compound and propose the hydrogen storage mechanism as $CoSi + H_2O + e \leftrightarrow [CoSi–H] + OH^-$. Liu et al. [20] prepare Co_2B alloys by both high temperature solid phase process and arc melting method, and the Co_2B alloys exhibit excellent electrochemical hydrogen storage behaviors. But there are seldom reports on the electrochemical performances of Co–P compounds. To the best of our knowledge, Cao et al. [21] obtain a reversible discharge capacity of 310 mAh g^{-1} for Co–P alloy by ball milling Co and P powers, and the reversible charge–discharge processes are attributed to the electrochemical storage and oxidation of hydrogen. But there is few detailed study on the electrochemical performances of crystallined Co–P compounds, so further investigations are worth to be made.

It is known that traditional solid state reaction has the advantages of high yield and easy operation, which is also introduced in the synthesis of Co–P compounds. The solid state methods to synthesize Co–P compounds could be divided into two types: one is to calcine Co metal and red phosphorous under inner atmospheres [22]; the other one is to reduce Co-based and phosphorus-based compounds under reducing atmospheres [23]. But the first one is difficult to obtain stoichiometric materials due to the volatilization and sublimation of red phosphorous, and the second one has potential safety hazard because of the adoption of H_2. Thus, simple and safe processes should be explored. Recently, Guan et al. [24] report a novel solid state reaction to synthesize a series of metal phosphide crystals using NaH_2PO_2 as reductant. But there are few similar reports on Co_2P, because many other Co–P compounds could be accreted with it, such as Co–P [25]. In this paper, we report a facile solid state synthesis of Co_2P crystal. We point out the appropriate conditions to synthesize pure Co_2P. The electrochemical performances of Co_2P explored as an anode material in alkaline rechargeable batteries are studied. Finally, the possible electrochemical mechanism is under detailed discussion.

* Corresponding author. Tel.: +86 22 23498089; fax: +86 22 23502604.
E-mail address: jiaolf@nankai.edu.cn (L. Jiao).

0925-8388/$ – see front matter © 2011 Elsevier B.V. All rights reserved.
doi:10.1016/j.jallcom.2011.09.029

2. Experimental

2.1. Preparation of Co_2P

Co_2P crystal was prepared successfully by a simple solid state reaction in accordance to the synthesis of Ni_2P [24]. In a typical reaction, 0.9 g $NaH_2PO_2 \cdot H_2O$ and 1.5 g $CoCl_2 \cdot 6H_2O$ were dissolved in 20 ml distilled water under continuous stir until a transparent solution was formed. The solution was placed in an oven and kept at 90 °C for 24 h to evaporate the water. The obtained pink material was ground, pressed into a pellet and calcined at 873 K for 6 h at a heating rate of 10 K min^{-1} in inert Ar atmosphere. Then the produced grayish-black material was washed with distilled water and ethanol to remove the residual ions. Finally, the wet products were dried in vacuum at 353 K for 12 h.

2.2. Structural and morphological characterization

The structure of the samples was characterized X-ray diffraction (XRD, Rigaku D/Max-2500, Cu Kα radiation, λ = 1.5418 Å) and energy dispersive X-ray spectra (EDS, ISIS300, Oxford, Instrument). The morphology was observed by scanning electron microscopy (SEM, Hitachi X-650).

2.3. Cell assembly

Electrochemical performances were evaluated in three-electrode test cell. The as-prepared material was made as working electrode, $NiOOH/Ni(OH)_2$ as counter electrode, Hg/HgO as reference electrode and 6 mol L^{-1} KOH solution as electrolyte. The working electrode was processed as follows: the as-prepared powers and nickel powders (mass ratio 1:3) were mixed homogeneously and pressed into a pellet (10 mm in diameter) under 30 MPa. Then the pellet was sandwiched between two foam nickel disks (20 mm in diameter) and pressed under 10 MPa. Finally, a nickel strip was soldered on the edge of the disk.

2.4. Electrochemical measurements

Galvanostatic charge/discharge measurements were operated on a Land CT2001A automatic battery tester. The electrodes were charged at 100 mA g^{-1} for 6 h and discharged at 50 mA g^{-1} to −0.5 V (vs. Hg/HgO). Cyclic voltammogram (CV) was recorded with a Zahner-Elektrik IM6e electrochemical workstation in the potential range of −1.2 V to −0.4 V at a scan rate of 0.2 mV s^{-1} at room temperature.

3. Results and discussion

3.1. Material characterization

Co_2P is successfully synthesized with a simple solid state reaction. The XRD patterns of the materials are shown in Fig. 1. Obviously, the mol ratio of NaH_2PO_2 to $CoCl_2$ is very important in synthesizing Co_2P crystal. When the mol ratio is 1:1, the major phase is $Na_2CoP_2O_7$. As it increases to 1.75:1, the diffraction peaks of $Na_2CoP_2O_7$ disappear and the major phase is Co_2P. Thus, pure Co_2P is obtained when the mol ratio is above 1.75:1, and the XRD pattern (Fig. 1d) is in good accordance with the standard Co_2P (JCPDS 65-2380) – orthorhombic system with a *Pnma* space group. The EDS pattern (shown in Fig. 2) indicates that the molar ratio of Co and P in the as-synthesized material is 0.3314:0.6686, confirming the stoichiometric ratio of Co_2P. SEM images of Co_2P (Fig. 3) exhibit that the particles are several hundred nanometers, and the particles aggregate to some extent.

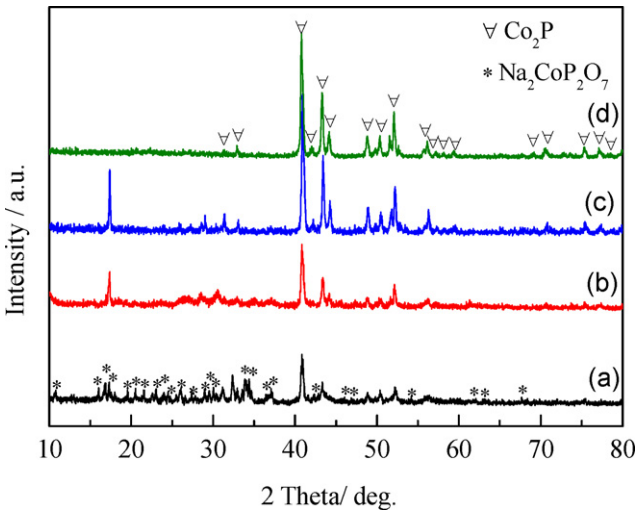

Fig. 1. XRD patterns of Co_2P synthesized with different mol ratios of $CoCl_2$ to NaH_2PO_2 (a) 1:1 (b) 1:1.25 (c) 1:1.5 (d) 1:1.75.

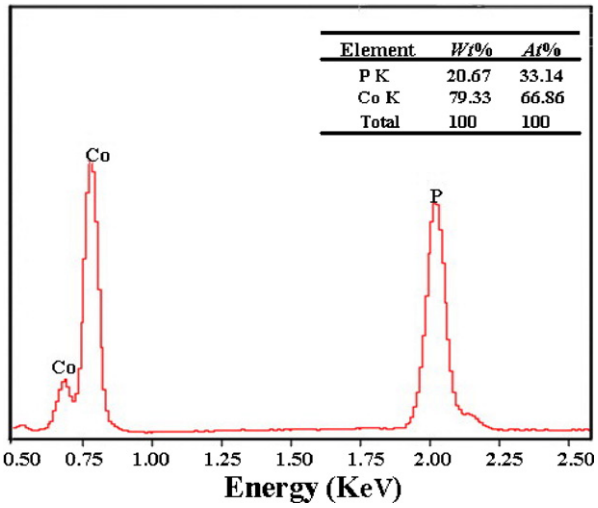

Fig. 2. EDS patterns of as-synthesized Co_2P crystal.

3.2. Galvanostatic discharge measurements

The discharge capacity curves for Co_2P electrode at a discharge current density of 50 mA g^{-1} at different cycles are shown in Fig. 4. It displays that all the discharge plateau potentials appear at about −0.8 V (vs. Hg/HgO), which is similar to the redox equilibrium potential of $Co/Co(OH)_2$ couple (−0.83 to −0.85 V) in alkaline solution [26]. Although the initial discharge capacity (107 mAh g^{-1}) is

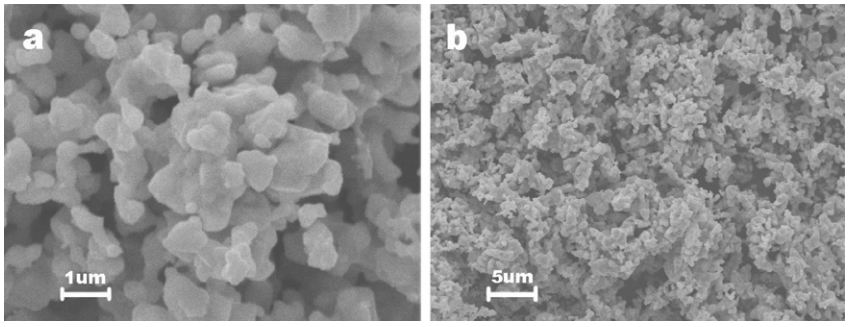

Fig. 3. SEM image of as-synthesized Co_2P crystal.

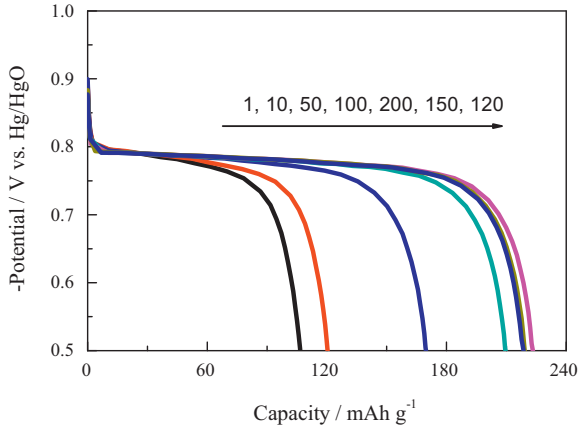

Fig. 4. Discharge capacity curves of Co_2P at the 1st, 10th, 50th, 100th 120th, 150th and 200th cycle.

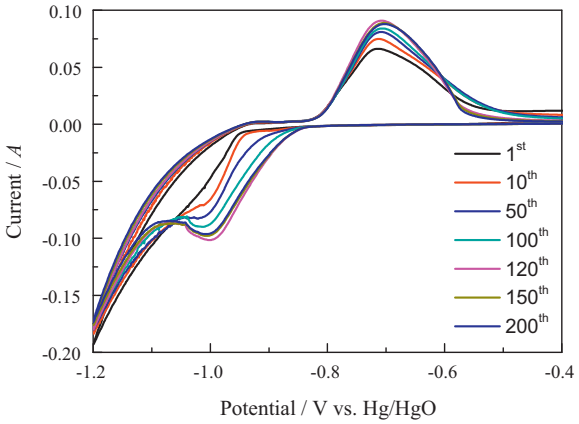

Fig. 6. CV curves of Co_2P materials at the 1st, 10th, 50th, 100th, 120th, 150th and 200th cycle. (For interpretation of the references to color in the artwork, the reader is referred to the web version of this article.)

low, it increases gradually to a maximum of 223.5 mAh g^{-1} in the 120th cycle then slightly decreases. The discharge capacity is 120.4, 169.7, 209.7, 223.5, 219.3 and 218.6 mAh g^{-1} at the 10th, 50th, 100th, 120th, 150th and 200th cycles, respectively.

The cyclic performance of as-synthesized Co_2P is shown in Fig. 5. Although there is a relative long activation cycle, the discharge capacity keeps increasing and reaches to the maximum (C_{max}) of 223.5 mAh g^{-1} at the 120th cycle. Besides, it displays high capacity retention, about 97.9% (C_{300}/C_{max}) at the 300th cycle. The long activation cycle may be attributed to that a relative strong interaction between P and Co in Co_2P crystal needs to overcome during cycling.

3.3. CV measurements

The CV curves of Co_2P electrode during different cycles are presented in Fig. 6. The pair of remarkable reduction–oxidation peaks appears at about −1.00 V and −0.70 V, respectively, similar to the potential plateaus of S–$Co(OH)_2$ and Co–BN materials reported by Wang [27] and Gao [28] group. As shown in Fig. 6, there are three important changes with the increase of cycle: (1) the pair of redox peak becomes more distinct, which indicates better redox reaction, (2) the peak currents become bigger, which indicates faster diffusivity, (3) the integral areas become larger, which indicates larger discharge capacities. These values keep increasing until to a maximum at the 120th cycle then with a slight decrease, which is consistent with the galvanostatic discharge curve results.

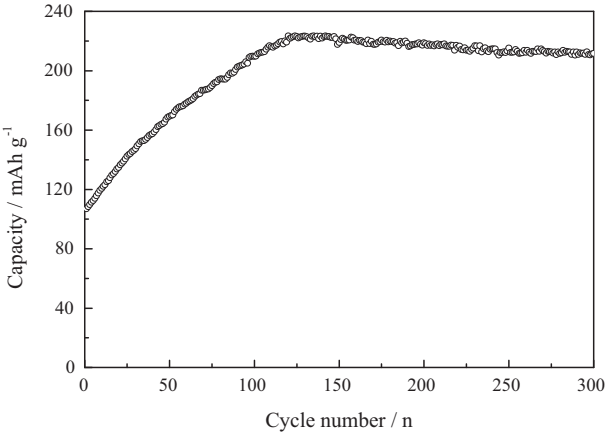

Fig. 5. Cyclic curve of Co_2P at the discharge current density of 50 mA g^{-1}.

3.4. Electrochemical mechanism

The possible electrochemical mechanism is investigated by CV (Fig. 6) and synchro XRD tests (Fig. 7) during different charge/discharge cycles.

In CV curves, a remarkable pair of redox peak is detected in every cycle, which testifies a redox mechanism. The curve shapes and peak potential locations are similar to those of Co [29] and $Co(OH)_2$ [30] electrodes, confirming a similar reversible reaction of Co_2P electrode as Co and $Co(OH)_2$ electrodes.

In order to further investigate the electrochemical mechanism, synchro XRD patterns during charge/discharge processes in different cycles are compared. As shown in Fig. 7, the diffraction peaks are all assigned to Co_2P crystal in the initial charging process. In the initial discharging process, the main phase is Co_2P but some weak diffraction peaks of $Co(OH)_2$ appear. In the 10th cycle, the main phase is also Co_2P, but some diffraction peaks of Co are detected in the charging process and $Co(OH)_2$ in the discharging process. In the 30th cycle, although the diffraction peaks of Co_2P are still high and strong, the diffraction peaks of Co and $Co(OH)_2$ become much stronger than in the 10th cycle in the corresponding charging/discharging process. Great changes occur in the 100th cycle, the diffraction peaks of Co_2P almost disappear, instead, all typical diffraction peaks are Co and $Co(OH)_2$. There are no typical

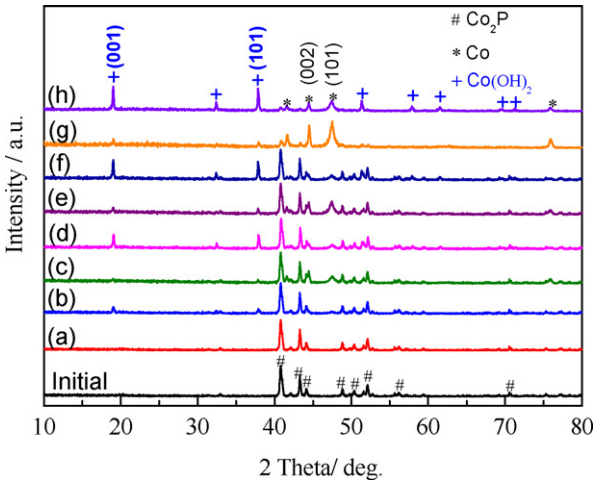

Fig. 7. XRD patterns of Co2P electrode at full charge and discharge state in different cycles (a, c, e, g – 1st, 10th, 30th and 100th charge cycle; b, d, f, h – 1st, 10th, 30th and 100th discharge cycle).

diffraction peaks of P-based materials detected in all the processes, because P may react with and dissolve in the dense 6 mol L^{-1} KOH solution during charge–discharge process.

Through the above analysis, we sum up a Faradaic redox mechanism expressed as follows:

$$Co_2P + 2OH^- \xrightarrow{\text{discharge}} Co(OH)_2 + Co + P + 2e \quad (1)$$

$$Co(OH)_2 + 2e \underset{\text{discharge}}{\overset{\text{charge}}{\rightleftarrows}} Co + 2OH^- \quad (2)$$

In the beginning, Co_2P converts to $Co(OH)_2$, Co and P through an irreversible reaction (1) during the discharging process. Meanwhile, the produced Co further converts to $Co(OH)_2$ through the reversible reaction (2) at the same discharge condition. But the reaction rate of (1) is slow due to a relatively strong interaction between Co and P in Co_2P. Also, inner Co_2P particles could not contact with the electrolyte, which results in an incomplete conversion of Co_2P in discharging process. As a result, Co_2P has a low initial discharge capacity and a long activation cycle. With the charge/discharge process going on, more and more Co_2P particles participate in reactions (1) and (2), which exhibits higher and higher discharge capacity. When the conversion occurs completely, the charge/discharge process becomes reversible which is due to a quasi-reversible redox reaction between $Co(OH)_2$ and Co [31], exhibiting a excellent discharge capacity. The generated P plays an important role in the electrochemical performances of Co_2P. With the reaction and dissolution of P, many new interspaces are brought into Co_2P body to enlarge the contact area between the active material and the electrolyte, which makes the conversion reaction of Co_2P easier and the redox reaction between Co and $Co(OH)_2$ faster.

4. Conclusions

Co_2P crystal is synthesized successfully with a facile solid-state reaction, in accordance to the synthesis of Ni_2P. The investigation on the reaction mechanism confirms that the molar ratio of NaH_2PO_2 to $CoCl_2$ and post-treatment with acid are necessary to synthesize pure materials. The maximum discharge capacity of Co_2P electrode is 223.5 mAh g^{-1} and capacity retention is 97.9% in the 300th cycle. The electrochemical mechanism is investigated by CV and synchro XRD tests during full charge/discharge processes. It confirms a quasi-reversible redox reaction between Co and $Co(OH)_2$ after the gradual conversion reaction of Co_2P in dense KOH electrolyte. The produced P could bring many interfaces after reacting with and dissolving in the electrolyte, which is important in enlarging the contact area between the active material and the electrolyte and making the electrochemical process easy. Co_2P would be a potential candidate as an anode material in alkaline rechargeable batteries, and it would be with great application prospect in such as catalyst and optoelectronics.

Acknowledgements

This work was financially supported by 973 program (2010CB631303), NSFC (51171083, 50971071, 51071087) and MOE Innovation Team (IRT-0927).

References

[1] P. Liu, J.A. Rodriguez, J. Am. Chem. Soc. 127 (2005) 14871.
[2] V. Zuzaniuk, R. Prins, J. Catal. 219 (2003) 85.
[3] S.T. Oyama, J. Catal. 216 (2003) 343.
[4] K. Senevirathne, A.W. Burns, M.E. Bussell, S.L. Brock, Adv. Funct. Mater. 17 (2007) 3933.
[5] A.W. Burns, K.A. Layman, D.H. Bale, M.E. Bussell, Appl. Catal. A: Gen. 343 (2008) 68.
[6] C. Stinner, Z. Tang, M. Haouas, T. Weber, R. Prins, J. Catal. 208 (2002) 456.
[7] A. Wang, L. Ruan, Y. Teng, X. Li, M. Lu, J. Ren, Y. Wang, Y. Hu, J. Catal. 229 (2005) 314.
[8] W. Li, B. Dhandapani, S.T. Oyama, Chem. Lett. 3 (1998) 207.
[9] J.A. Cecilia, A. Infantes-Molina, E. Rodriguez-Castellon, A. Jimenez-Lopez, Appl. Catal. B: Environ. 92 (2009) 100.
[10] J.A. Cecilia, A. Infantes-Molina, E. Rodriguez-Castellon, A. Jimenez-Lopez, J. Catal. 263 (2009) 4.
[11] N. Singh, P.K. Khanna, P.A. Joy, J. Nanopart. Res. 11 (2009) 491.
[12] H. Kleinke, H.F. Franzen, J. Alloys Compd. 255 (1997) 110–116.
[13] M. Cortes, E. Gomez, E. Valles, J. Solid State Electrochem. 14 (2010) 2225.
[14] S.L. Brock, K. Senevirathne, J. Solid State Chem. 181 (2008) 1552.
[15] J. Park, B. Koo, K.Y. Yoon, Y. Hwang, M. Kang, J.-G. Park, T. Hyeon, J. Am. Chem. Soc. 127 (2005) 8433.
[16] J. Wang, Q. Yang, J. Zhou, K. Sun, Z. Zhang, X. Feng, T. Li, Nano Res. 3 (2010) 211.
[17] M. Mitov, A. Popov, I. Dragieva, J. Appl. Electrochem. 29 (1999) 59.
[18] Q. Wang, L. Jiao, H. Du, W. Peng, S. Liu, Y. Wang, H. Yuan, Int. J. Hydrogen Energy 35 (2010) 8357.
[19] G. He, L.-F. Jiao, H.-T. Yuan, Y.-Y. Zhang, Y.-J. Wang, Electrochem. Commun. 8 (2006) 1633.
[20] Y. Liu, Y.J. Wang, L.L. Xiao, D.W. Song, L.F. Jiao, H.T. Yuan, Electrochem. Commun. 9 (2007) 925.
[21] Y.L. Cao, W.C. Zhou, X.Y. Li, X.P. Ai, X.P. Gao, H.X. Yang, Electrochim. Acta 51 (2006) 4285.
[22] S.K. Jain, S. Kumar, P.S.R. Krishna, A.B. Shinde, A. Krishnamurthy, B.K. Srivastava, J. Alloys Compd. 439 (2007) 13.
[23] J. Gopalakrishnan, S. Pandey, K.K. Rangan, Chem. Mater. 9 (1997) 2113.
[24] Q. Guan, W. Li, M. Zhang, K. Tao, J. Catal. 263 (2009) 1.
[25] M.D. Silva, U. Klement, J. Microsc. 228 (2007) 338.
[26] A. Durairajan, B.S. Haran, B.N. Popov, R.E. White, J. Power Sources 83 (1999) 114.
[27] D.W. Song, Y.J. Wang, Q.H. Wang, Y.P. Wang, L.F. Jiao, H.T. Yuan, J. Power Sources 195 (2010) 7115.
[28] Z.W. Lu, S.M. Yao, G.R. Li, T.Y. Yan, X.P. Gao, Electrochim. Acta 53 (2008) 2369.
[29] S.R. Chung, K.W. Wang, P. Perng, J. Electrochem. Soc. 153 (2006) A1128.
[30] S. Hana, Z. Feng, L. Hu, Y. Li, J. Hao, J. Zhang, Mater. Chem. Phys. 124 (2010) 17.
[31] P. Elumalai, H.N. Vasan, N. Munichandraiah, J. Power Sources 93 (2001) 201.